sciendo

Polish Journal of Medical Physics and Engineering
The Journal of Polish Society of Medical Physics
ISSN 1898-0309, doi: 10.2478/pjmpe-2025-0022

September 2025
Vol 31, Issue 3

Scientific Paper

Comparative Evaluation of Metal Artifact Reduction Algorithms in Computed Tomography: Siemens iMAR vs. GE MARS for Improved Radiotherapy Planning

Kamila Rawojć[1,ACD], Karolina Nowosad[2,BCD], Bartosz Kiełtyka[3,E], Anna Pędracka[4,E], Łukasz Brandt[4,E], Anna Dziecichowicz[1,C], Mansoor M. Ahmed[5,EF], Kamil Kisielewicz[1,ACDF,*]

[1]*Medical Physics Department, Maria Sklodowska-Curie National Research Institute of Oncology, Kraków, Poland*
[2]*Faculty of Physics and Applied Computer Science, AGH, Kraków, Poland*
[3]*Department of Medical Physics, The University Hospital, Jagiellonian University, Kraków, Poland*
[4]*Department of Health Sciences, Jagiellonian University, Collegium Medicum, Kraków, Poland*
[5]*Albert Einstein College of Medicine, Montefiore Einstein, New York, USA*
**Corresponding author: Kamil Kisielewicz1; z5kisiel@cyf-kr.edu.pl*

(received 6 December 2024; revised 10 February 2025, 11 March 2025, 12 June; accepted 15 June 2025)

Abstract

Introduction: In this article, the effectiveness of two commercial metal artifact reduction algorithms, Siemens iMAR and GE MARS, in computed tomography (CT) imaging is evaluated. Metal artifacts, which arise primarily due to the presence of high atomic number metals in clinical imaging, significantly degrade image quality and impede accurate diagnostics.

Material and methods: The study compares monoenergetic and dual-energy CT reconstruction algorithms by examining their performance on phantom models, including a Gammex Tissue Characterization Phantom and a custom-made spine stabilization system phantom. Quantitative assessments, such as Hounsfield unit analysis were performed.

Results: The results show that the iterative reconstruction algorithm (iMAR) from Siemens offers superior artifact suppression and image clarity compared to GE's dual-energy algorithm (MARS), particularly in cases involving titanium implants. Quantitative assessments, such as Hounsfield unit measurements and visual image analysis, confirm that iMAR produces images with reduced artifacts and more consistent tissue characterization.

Conclusions: These findings suggest that the choice of artifact reduction algorithm has a profound impact on the diagnostic and planning accuracy of CT scans in patients with metal implants.

Keywords: Artifacts, MARS, iMAR, GE Discovery CT, Siemens

Introduction

In radiotherapy treatment planning, high-quality imaging is essential to ensure precise tumor localization and the accurate delineation of target volumes, while safeguarding surrounding healthy tissues. Computed Tomography (CT) remains the primary imaging modality for this purpose, providing the foundational anatomical information needed to design effective radiotherapy protocols. However, the presence of metallic implants i.e. dental restorations, surgical clips, and orthopedic hardware, introduces significant challenges in the form of metal artifacts, which can distort CT images. These artifacts, characterized by streaking and shadowing, compromise the clarity and accuracy of CT scans, ultimately hindering the reliability of radiotherapy planning. The impact of these distortions can result in suboptimal dose distribution, potentially leading to either underdosing of the tumor or overdosing of adjacent healthy structures, which could negatively affect patient outcomes[1-4].

To address the issue of metal artifacts in CT imaging, several advanced metal artifact reduction (MAR) algorithms have been developed in recent years. Among the most widely adopted are Siemens iterative Metal Artifact Reduction (iMAR) and GE's Metal Artifact Reduction System (MARS). These algorithms are designed to reduce the severity of metal-induced distortions, improving image quality and diagnostic accuracy. Siemens iMAR, an iterative reconstruction algorithm, works by identifying metal objects within the scan, correcting for beam-hardening effects, and reprocessing the data iteratively to remove artifacts. Similarly, GE MARS employs sophisti-

© 2025 Authors This is an open access article licensed under the Creative Commons Attribution-NonCommercial-NoDerivs License (http://creativecommons.org/licenses/by-nc-nd/4.0/).

Authors' contribution: A – Research concept and design, B – Collection and/or assembly of data, C – Data analysis and interpretation, D – Writing the article, E – Critical revision of the article, F – Final approval of the article.

cated image processing techniques to reduce streaking and shading caused by metallic objects. Both algorithms have shown promise in clinical applications, yet their comparative performance in the specific context of radiotherapy planning remains underexplored[4-7].

Recent studies highlight the critical role of MAR algorithms in clinical settings, where they have demonstrated improvements in image quality and diagnostic confidence. A 2022 study by Gnanasambandam et al.[3] showed that implementing iMAR in CT imaging improved diagnostic confidence in patients with metallic implants, particularly in regions with critical anatomy such as the head and neck, where radiotherapy accuracy is paramount. Similarly, Murazaki et al. (2019)[8] demonstrated that GE's MARS algorithm improved image quality and reduced artifacts significantly in spinal CT scans, where metallic implants are often present due to neurologic interventions. However, direct comparisons between Siemens iMAR and GE MARS in terms of radiotherapy planning remain scarce, creating a gap in our understanding of which algorithm may offer superior performance in this highly specialized application[2,8].

The primary aim of this study is to conduct a comparative evaluation of Siemens iMAR and GE MARS in reducing metal artifacts in CT images used for radiotherapy planning. This study focuses on assessing their impact on diagnostic accuracy, tumor delineation, and dose distribution to enhance image clarity and minimize treatment uncertainties.

The study will also evaluate the ability of these algorithms to enhance image clarity in the presence of metallic implants and how these improvements translate to more precise radiotherapy treatment planning. Improved accuracy in contouring target volumes can lead to more precise radiation dose delivery, reducing the risk of damaging healthy tissues and increasing the potential for tumor control.

The influence of these findings on radiotherapy treatment modification is significant. Enhanced image quality through effective MAR algorithms allows for better visualization of tumor margins and critical organs at risk (OARs)[3,10,11]. This, in turn, facilitates more accurate dose calculation and distribution, particularly in intensity-modulated radiation therapy (IMRT), volumetric-modulated arc therapy (VMAT) and stereotactic body radiation therapy (SBRT), where precision is crucial. As noted by Gnanasambandam et al. (2022)[3], improvements in CT image quality can reduce the risk of radiation-induced side effects by optimizing the sparing of healthy tissues while ensuring adequate tumor coverage. Moreover, accurate imaging minimizes uncertainties in dose distribution, allowing clinicians to confidently escalate doses in areas where necessary, potentially improving local control in glioblastoma, head and neck cancers, and pelvic malignancies[12-14].

By providing a detailed comparison between Siemens iMAR and GE MARS, this study will contribute to the growing body of knowledge on how advanced imaging algorithms can improve radiotherapy outcomes. In particular, the findings will offer insights into which algorithm may be preferable for specific clinical scenarios involving metallic implants, thereby assisting clinicians in selecting the best technology for their patients. The ultimate goal is to ensure that technological innovations in CT imaging continue to support advancements in personalized, precision radiotherapy.

Materials and Methods

Imaging protocols were selected to ensure optimal artifact reduction for each system. The Siemens iMAR algorithm (version VA48A) was applied using the "dental fillings" setting within its iterative reconstruction framework, while the GE MARS algorithm (software version 30.0) utilized the "body medium – FBP" setting. The scanning parameters were as follows:

- **GE Discovery 750HD**: kV: dual kV acquisition - GSI (GemStone Imaging), helical acquisition (pitch 0.984), 512 x 512 matrix, slice thickness: 0.625 mm, detector coverage: 40 mm, CDTIvol: 17.8 mGy.
- **Siemens SOMATOM Definition AS**: kV: 120 , helical acquisition (pitch 0.95), 512 x 512 matrix, slice thickness: 0.6 mm, Acquisition: 16 × 1.2, iMAR settings: "dental fillings" iterative reconstruction, CDTIvol: 17.2 mGy, CareDose: off.

The acquisitions were performed at similar dose levels to ensure comparability. The CTDIvol was 17.8 mGy for the GE scanner and 17.2 mGy for the Siemens scanner. The reconstructed slice widths were also comparable (0.625 mm for GE and 0.6 mm for Siemens).

Equipment and Imaging Protocols:
Siemens SOMATOM Definition AS: The scanner was equipped with iMAR, an iterative algorithm designed to reduce metal-induced artifacts. Imaging was performed with a single X-ray tube generating single energy spectrum with a tube potential of 120 kVp, optimized for tumor localization and organ delineation in radiotherapy planning.

GE Discovery 750HD (spectral CT): This scanner employed MARS, a multi-energy spectral CT-based algorithm for metal artifact reduction. Dual kV acquisition was used (GSI), with simultaneous 80 kVp and 140 kVp beams to improve tissue characterization. This system is known for enhanced contrast resolution and metal artifact suppression. The images analyzed in this study were obtained from the original 80 kVp and 140 kVp summed up by the reconstruction algorithm – so called GSI, without the application of virtual monoenergetic imaging.

Phantoms

Two phantoms were utilized for image acquisition:

1. Gammex Tissue Characterization Phantom Model 467: The phantom simulated various tissue densities and included a titanium implant to mimic clinical scenarios involving metal artifacts.

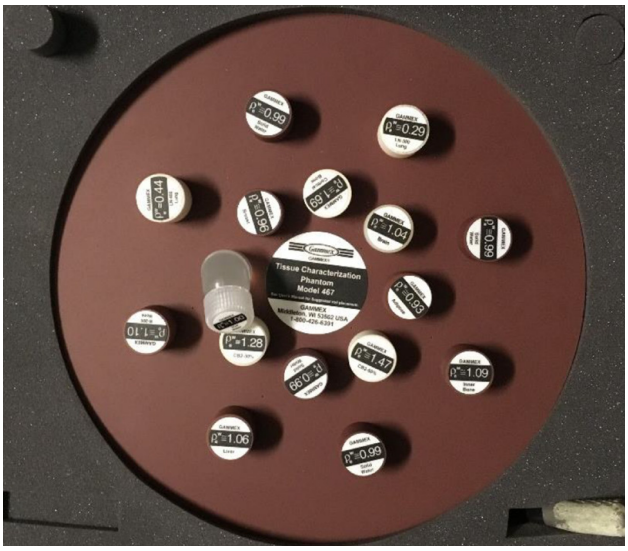


Figure 1. Gammex Tissue Characterization Phantom Model 467.

2. Custom Spine Stabilization Phantom: The phantom designed to replicate the geometry of a spinal stabilization system, created using gelatin and a titanium rod to assess the algorithms' performance in a more complex metal geometry scenario.

The analyzed images correspond exactly to **Figures 3, 4, 5**, and **6**. Images were evaluated using a 1-5 Likert scale, where **artifact visibility** refers to the extent to which metal artifacts obscure phantom internal structures, so called - anatomical structures, and **clarity** refers to the sharpness and contrast of the reconstructed images. Observers assessed these factors independently. Image analysis: Visual and Quantitative

Five experienced radiologists independently evaluated the images for the presence and extent of metal artifacts, using a 5-point Likert scale to assess clarity and artifact reduction.

For Gammex phantom, Hounsfield unit (HU) values were measured in regions of interest (ROIs) within each insert. The average HU values and standard deviations were calculated for both soft tissues and metal-affected regions. Statistical comparisons were made between images acquired with and without the artifact reduction algorithms for each scanner. The primary outcome was the reduction of metal artifacts, quantified as the difference in HU variability and clarity of anatomical structures (internal structures of the phantom), including soft tissues, bony structures, and metal implants, were assessed for clarity and visibility.

Custom spine stabilization phantom has not been quantitatively analysed.



Figure 2. Custom Spine Stabilization Phantom (transversal and sagittal views).

Image Acquisition

Images of the phantoms were acquired on both scanners using standard clinical protocols for head-and-neck radiotherapy planning. Scans were performed under identical conditions with and without metal implants for both phantoms. Each scanner applied its respective artifact reduction algorithm (iMAR for Siemens and MARS for GE) after baseline imaging without artifact reduction.

Statistical Analysis

Statistical analysis was conducted using paired t-tests to compare HU values across different scanners and reconstruction algorithms. A significance level of $\mathbf{p < 0.05}$ was applied. Interobserver agreement was assessed using **Cohen's kappa coefficient** to evaluate consistency in visual scoring.

The calibration curve analysis

The calibration curve analysis was conducted to examine the relationship between Hounsfield Units (HU) and Relative Electron Density (RED) across different reconstruction algorithms. The analysis was performed under four conditions:

1. Reference phantom without metal artifact reduction.
2. Reference phantom reconstructed with iMAR or MARS.
3. Phantom with a titanium insert, without metal artifact reduction.
4. Phantom with a titanium insert, reconstructed with iMAR or MARS. This analysis serves as a **quantitative visualization tool** to assess reconstruction accuracy.

This methodology allowed for a comprehensive evaluation of Siemens iMAR and GE MARS in reducing metal artifacts in CT images, improving accuracy in radiotherapy planning in special conditions.

Results

Visual Analysis of Gammex Tissue Characterization Phantom

The visual assessment was performed on CT images of the Gammex phantom acquired using two systems: the Siemens SOMATOM Definition AS with iMAR and the GE Discovery 750HD with multi-energy MARS. Images were evaluated for artifact visibility and clarity using a 1–5 Likert scale by five independent observers (1 = poor, 5 = excellent). The Window Level (WL) and Window Width (WW) were standardized across both scanners, set at 500 and 2385, respectively.

The results indicated that images reconstructed with Siemens iMAR algorithm demonstrated significantly fewer artifacts and higher clarity scores compared to those obtained using GE's MARS algorithm (**Figures 3 and 4**). For scans without the titanium implant, the iMAR algorithm achieved average clarity and artifact reduction scores of 4.8 and 4.6, respectively, while MARS scored 3.6 and 3.4. In scans with the titanium insert, iMAR scores were 4.2 for clarity and 4.0 for artifact reduction (**Table 1**), compared to 2.0 and 2.2 for MARS (**Table 2**).

Table 1. Mean observer score: Siemens and Gammex phantom.

	no titanium insert, no iMAR	no titanium insert, iMAR	titanium insert, no iMAR	titanium insert, iMAR
Artifacts	4,4	4,6	2,6	4,0
Clarity	4,8	4,8	3,8	4,2

Table 2. Mean observer score: GE and Gammex phantom.

	no titanium insert, no MARS	no titanium insert, MARS	titanium insert, no MARS	titanium insert, MARS
Artifacts	3,4	3,4	1,8	2,2
Clarity	3,6	3,2	2,0	2,0

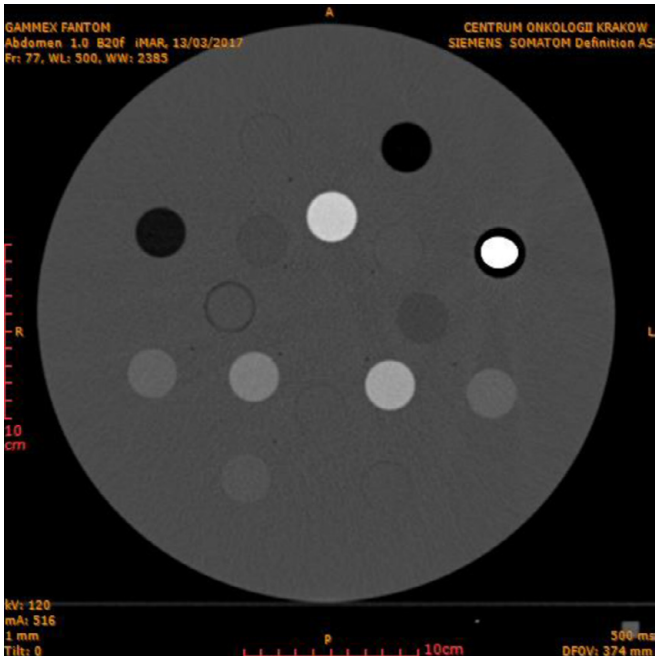


Figure 3. Image of Gammex Tissue Characterization Phantom Model 467 with titanium insert – iMAR reconstruction.

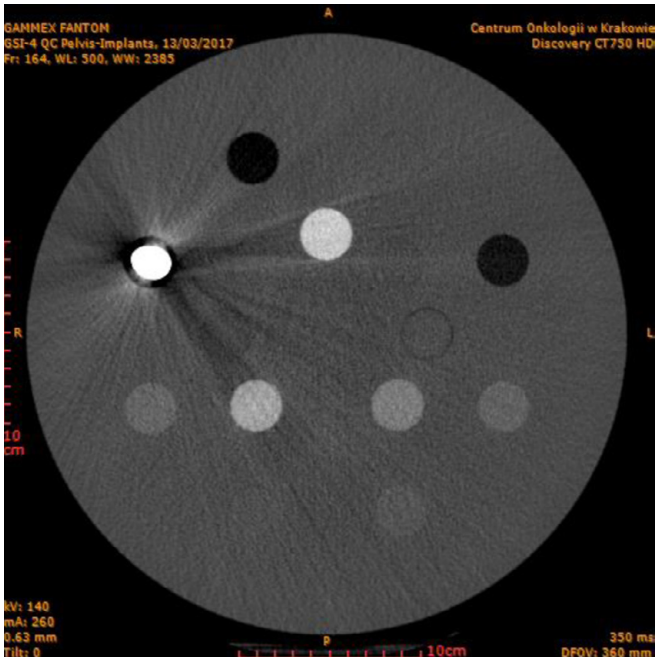


Figure 4. Image of Gammex Tissue Characterization Phantom Model 467 with titanium insert – MARS reconstruction.

Quantitative Analysis of Gammex Tissue Characterization Phantom images

Quantitative evaluation involved measuring Hounsfield Unit (HU) values and standard deviations across regions of interest (ROIs) in various phantom materials (inserts). The mean HU differences between reference images and adjacent slices reconstructed with iMAR remained within 1% for most tissues, indicating minimal deviation. Conversely, images processed using MARS exhibited mean HU variations of up to 25%, deviating substantially from the reference.

Standard deviations of HU values for iMAR images were consistently lower compared to those for MARS, especially in scans with the titanium insert, where MARS demonstrated up to threefold higher variability than iMAR – **Table 3**. Mean SD for IMAR reconstruction is **25.42** vs. **73.73** for MARS.

Table 3. HUs and SDs for different Gammex Tissue Characterization Phantom inserts.

Phantom insert	iMAR mean HU	iMAR SD	MARS mean HU	MARS SD
Solid water (PMMA)	-1,12	21,34	23,20	56,03
LN-300 lung	-719	33,37	-663,15	72,37
Inner bone	198,07	23,32	222,86	66,73
Liver	68,56	21,72	72,60	56,68
B-200 bone	202,93	21,67	207,05	59,39
LN-450 lung	-529,35	26,38	-502,08	62,02
Breast	-43,06	23,01	-11,67	68,76
Cortical bone	1161	33,82	1116	89,43
Brain	20,89	22,82	22	100,61
Adipose	-87,21	22,74	-107,28	82,67
CB2-50%	778	29,04	751,29	91,29
CB-30%	425,73	25,83	416	78,72

Cortical bone, brain and ln-450 lung are closest to the metallic insert.

Visual Analysis of Custom spine stabilization phantom

Table 4. Mean observer score for custom spine stabilization phantom (averaged values).

	GE - no MARS	GE -MARS	Siemens – no iMAR	Siemens – iMAR
Artifacts	1,9	2,3	2,5	3,8
Clarity	2.0	2,4	3,7	4,0

Validation Using a Custom Spine Stabilization Phantom

The findings were validated using a custom spine stabilization phantom, confirming the superior performance of the iMAR algorithm. Images reconstructed with iMAR consistently exhibited fewer artifacts and higher quality scores, particularly in regions near titanium elements (**Figures 5 and 6**).

Calibration Curve Analysis (HU vs. RED)

Calibration curves depicting the relationship between HU and Relative Electron Density (RED) were analyzed for each CT system under four conditions, described in material and methods.

It was noticed that for the Siemens scanner, the HU values obtained for a given value of rel. electron density (RED), obtained from 4 reconstructions, are much closer to each other comparing to the GE device. Analyzing the graphs (**Figure 7**)



Figure 5. Custom spine stabilization phantom – iMAR reconstruction.



Figure 6. Custom spine stabilization phantom – MARS reconstruction.

of the Siemens scanner, it was found that three of the four compared measurement combinations overlap. There is a visible shift in the values obtained for the phantom with an endoprosthesis (titanium insert) using the basic CT reconstruction algorithm. The results for the highest insert densities (ribs, CB2-50%) are shifted to the left in relation to the remaining measurements (HU values are lower), while for the lowest (lungs) - to the right (HU values are higher).

The calculated uncertainties are small in relation to the measured values and mostly within the limit of ~2 HU. For large HU values (over 800 HU), the uncertainties increase up to 3.7 HU (53 HU for GE scanner). However, considering the

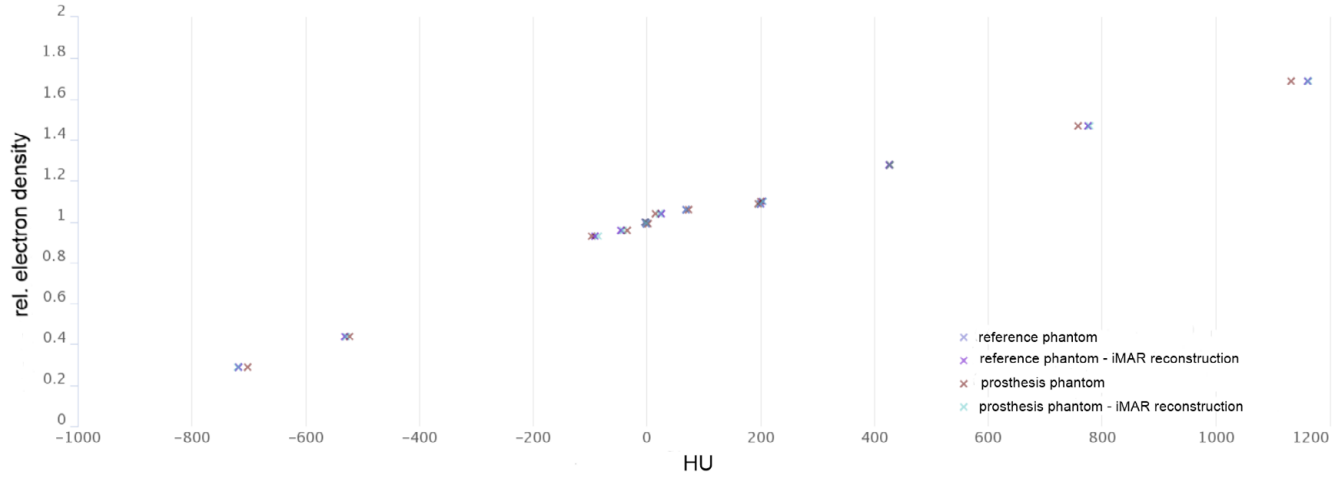


Figure 7. Treatment planning system (TPS) calibration curves for Siemens CT scanner.

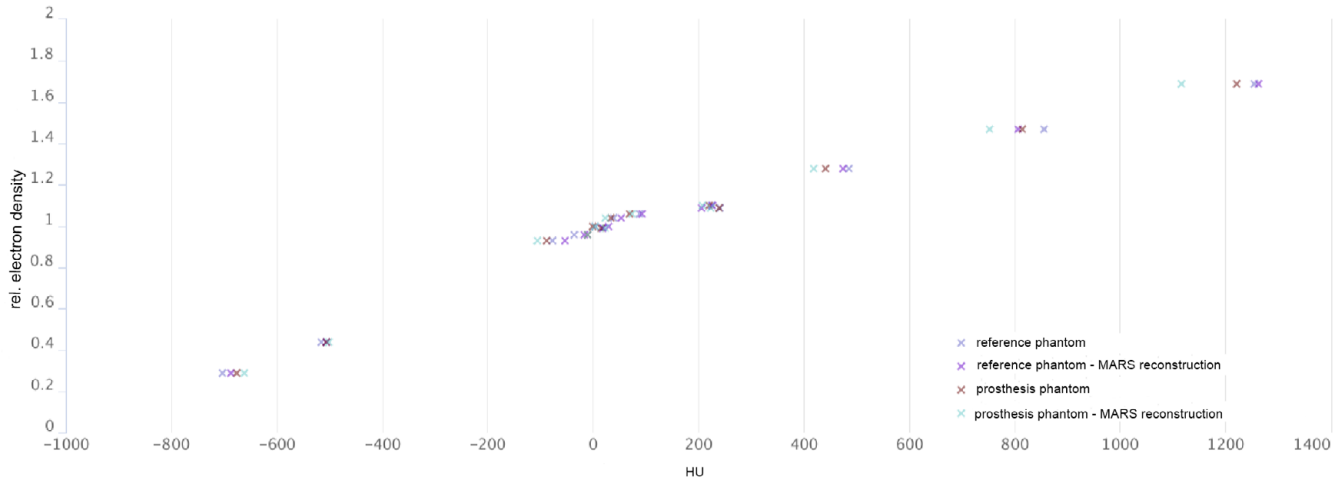


Figure 8. Treatment planning system (TPS) calibration curves for GE CT scanner

scale we use, these are still small values (0.32% in relation to the largest average HU).

In the case of GE scanner, average HU value and the standard deviation for the reference phantom with the basic reconstruction and multi-energy MARS reconstruction, it was noticed that most of the results fluctuate within the range of up to 25% (**Figure 8**). Standard deviations for measurements using the MARS reconstruction algorithm, both with and without endoprosthesis (titanium insert), are higher than for the results obtained with the basic CT reconstruction.

Statistical analysis confirmed that **HU differences between Siemens iMAR and GE MARS were statistically significant ($p < 0.05$), with iMAR demonstrating lower HU variability and greater consistency in soft tissue and titanium regions**

Comparing the results and graphs for both scanners, it can be seen that the values obtained for the single-energy Siemens Somatom AS CT scanner are less divergent than for the multi-energy GE Discovery 750 HD CT scanner. The values obtained in the studies using the single-energy iterative iMAR metal artifact reconstruction algorithm practically match the results obtained for the reference phantom. Unfortunately, the measurements obtained using the multi-energy MARS metal artifact reconstruction algorithm show significant deviations from the reference values, with noticeable discrepancies across different combinations.

Conclusions

The comparative evaluation of metal artifact reduction algorithms—Siemens iMAR and GE MARS—highlights notable differences in their effectiveness when applied to computed tomography imaging of phantoms with high-density implants. The findings show that the Siemens iMAR algorithm consistently provides superior results in terms of artifact suppression and maintaining accurate Hounsfield Unit (HU) values, as compared to the multi-energy MARS algorithm by GE.

The superiority of iMAR is evident both visually and quantitatively. Visual assessment showed significantly fewer artifacts and improved clarity in images processed with iMAR, particularly in complex cases involving the spine stabilization phantom. This observation is consistent with recent studies such as those by Kim et al. (2019)[5] and Li et al. (2023)[7], which underscore the advantages of iterative reconstruction methods

in reducing artifacts and maintaining diagnostic accuracy in radiotherapy planning.

Quantitative analysis further supports these findings, revealing that HU variability in iMAR-reconstructed images was considerably lower than in those processed using MARS. This aligns with the conclusions drawn by Ziemann et al. (2018)[9], who emphasized the importance of reducing HU variability for accurate dose calculation in radiotherapy. The smaller deviation of HU values in iMAR-treated images, particularly in scans involving titanium inserts, suggests its robustness in managing the complex attenuation properties of metals.

In contrast, the GE MARS algorithm, despite its spectral imaging capabilities, demonstrated higher variability in HU values and less effective artifact reduction. Studies such as those by Hansen et al. (2017)[10] and Rousselle et al. (2020)[11] also highlight the limitations of dual-energy systems when dealing with intricate metal artifacts. The findings in this study support the notion that while spectral imaging can offer benefits in certain contexts, it may not be sufficient for scenarios involving complex metallic structures.

To conclude: quantitative assessments, such as Hounsfield unit measurements and visual image analysis, confirm that iMAR produces images with reduced artifacts and more consistent tissue characterization. These findings suggest that the choice of artifact reduction algorithm has a profound impact on the diagnostic and planning accuracy of CT scans in patients with metal implants.

Discussion

The clinical implications of these findings are significant for radiotherapy, where accurate imaging near metallic implants is crucial for precise tumor delineation and dose distribution. Using effective artifact reduction methods like iMAR can enhance the quality of radiotherapy plans, potentially leading to better patient outcomes. This perspective is echoed in the work of Rousselle et al. (2020)[11], who noted that improved imaging precision translates to more effective treatment planning in clinical oncology.

A direct comparison of MAR algorithms on the same raw data is not possible due to proprietary constraints, we clarify that this study evaluates their performance under comparable conditions. Differences in scanner technology and acquisition parameters have been discussed as potential confounding factors. We also highlight that detector technology and system geometry may contribute to the observed variations in image quality.

Future research should focus on exploring hybrid approaches that integrate iterative methods like iMAR with spectral imaging to leverage the strengths of both. Studies such as those by Ziemann et al., Li et al., Glide et al.[9-14] have suggested that such combined approaches may further enhance the capability to manage metal artifacts in a clinical setting. Additionally, expanding the investigation to other types of high-density materials, such as dental implants and orthopedic hardware, could provide further insights into the versatility and robustness of these algorithms.

References

1. Giantsoudi D, De Man B, Verburg J, et al. Metal artifacts in computed tomography for radiation therapy planning: dosimetric effects and impact of metal artifact reduction. Phys Med Biol. 2017;62(8)-R80. doi: 10.1088/1361-6560/aa5293
2. Puvanasunthararajah S, Fontanarosa D, Wille ML, et al. The application of metal artifact reduction methods on computed tomography scans for radiotherapy applications: A literature review. J Appl Clin Med Phys. 2021;22(6):198-223. doi: 10.1002/acm2.13255
3. Gnanasambandam A, Raj NAN, Sollinselvan K. Effects of metal implants and validation of four treatment planning methods used for radiotherapy dose calculation. Rep Pract Oncol Radiother. 2022;27(5):821-831. doi: 10.5603/RPOR.a2022.0098
4. Schwahofer A, Bär E, Kuchenbecker S, et al. The application of metal artifact reduction (MAR) in CT scans for radiation oncology by monoenergetic extrapolation with a DECT scanner. Z Med Phys. 2015;25(4):314-325. doi: 10.1016/j.zemedi.2015.05.004
5. Kim C, Pua R, Lee CH, et al. An additional tilted-scan-based CT metal-artifact-reduction method for radiation therapy planning. J Appl Clin Med Phys. 2019;20(1):237-249. doi: 10.1002/acm2.12523
6. Andersson KM, Dahlgren CV, Reizenstein J, et al. Evaluation of two commercial CT metal artifact reduction algorithms for use in proton radiotherapy treatment planning in the head and neck area. Med Phys. 2018;45(10):4329-4344. doi: 10.1002/mp.13115
7. Li B, Huang J, Ruan J, et al. Dosimetric impact of CT metal artifact reduction for spinal implants in stereotactic body radiotherapy planning. Quant Imaging Med Surg. 2023;13(12):8290-8302. doi: 10.21037/qims-23-442
8. Murazaki H, Fukunaga J, Hirose TA, et al. Dosimetric assessment of a single-energy metal artifact reduction algorithm for computed tomography images in radiation therapy. Radiol Phys Technol. 2019;12(3):268-276. doi: 10.1007/s12194-019-00517-7
9. Ziemann C, Stille M, Cremers F, et al. Improvement of dose calculation in radiation therapy due to metal artifact correction using the augmented likelihood image reconstruction. J Appl Clin Med Phys. 2018;19(3):227-233. doi: 10.1002/acm2.12325
10. Hansen CR, Christiansen RL, Lorenzen EL, et al. Contouring and dose calculation in head and neck cancer radiotherapy after reduction of metal artifacts in CT images. Acta Oncol. 2017;56(6):874-878. doi: 10.1080/0284186X.2017.1287427
11. Rousselle A, Amelot A, Thariat J, et al. Metallic implants and CT artefacts in the CTV area: Where are we in 2020? Cancer Radiother. 2020;24(6-7):658-666. doi: 10.1016/j.canrad.2020.06.022
12. Maerz M, Mittermair P, Krauss A, et al. Iterative metal artifact reduction improves dose calculation accuracy: Phantom study with dental implants. Strahlenther Onkol. 2016;192(6):403-413. doi: 10.1007/s00066-016-0958-z
13. Glide-Hurst C, Chen D, Zhong H, Chetty IJ. Changes realized from extended bit-depth and metal artifact reduction in CT. Med Phys. 2013;40(6):061711. doi: 10.1118/1.4805102
14. Li H, Noel C, Chen H, et al. Clinical evaluation of a commercial orthopedic metal artifact reduction tool for CT simulations in radiation therapy. Med Phys. 2012;39(12):7507-7517. doi: 10.1118/1.4762814